

# Air entrainment and energy dissipation on stepped spillways downstream of piano key weirs

Rogério de Castilho de Paula Gomes

Supervisors:

Prof. Dr. Jorge de Saldanha Gonçalves Matos  
Dr. Maria Teresa Fontelas dos Santos Viseu

Instituto Superior Técnico, Lisbon, Portugal  
December 2017

## Abstract

The present study is focussed on the skimming flow on a stepped spillway downstream of a piano key weir (PKW), as well as on the hydraulic jump on its adjacent stilling basin.

The experimental study took place at the National Laboratory of Civil Engineering (LNEC). Therein air concentration data were acquired along the stepped spillway, and piezometric head data measured on the stilling basin floor.

Along the stepped spillway, air concentration distribution, mean air concentration, equivalent clear water depth and characteristic flow depths were analysed. The results indicate that the mean air concentrations obtained along the stepped spillway downstream of a piano key weir with 4 cm high steps are slightly lower than those obtained with 8 cm high steps.

For the stilling basin, the distribution of the piezometric head at the initial section and the development of the piezometric head along the stilling basin were analysed. Based on the piezometric head, the equivalent clear water depth, the residual specific energy and the total energy dissipation at the spillway were analysed. The results indicate that the total energy dissipation for the stepped spillway downstream of a piano key weir with 4 cm high steps is slightly lower than those obtained with 8 cm high steps. Also, the total energy dissipation in the chute with a PKW weir is slightly lower than that in the chute with a WES weir.

Finally, normalized formulae are presented to estimate the head loss on stepped spillways downstream of PKW or WES weirs.

**Keywords:** stepped spillway, piano key weir (PKW), skimming flow, air entrainment, stilling basin, energy dissipation.

## 1. Introduction

Dams play an important role in the development of countries, being responsible for flood control, hydroelectric energy, water storage for human consumption and agricultural purposes, among others. The design of a dam must ensure the safety of the dam throughout its lifetime. With the increase in hydrological knowledge, as a result of larger data series, as well as due to climate change effects, namely regarding extreme meteorological phenomena, the update of the design flows for many existing dams is of clear importance, in order to ensure safe flood release by the dam spillway. Thus, the adopted solution may involve increasing the flow capacity of existing spillways, notably through rehabilitation of the existing weirs for more hydraulic efficient solutions. In these cases, a current solution is to use labyrinth weirs, or, more recently, piano key weirs. The piano key weir, first developed by Hydrocoop, has been considered hydraulically more efficient than the labyrinth weir, with the advantage to the latter of easier installation on the top of gravity dams.

The present study was conducted in a facility assembled at the National Laboratory of Civil Engineering (LNEC), in Lisbon, Portugal, in the framework of previous studies conducted in the same facility. Previous research studies conducted in this experimental facility include the PhD thesis developed by Matos (1999), in which the experimental facility used in the present work was idealized and materialized, as well as the thesis by Meireles (2004, 2011), Renna (2004) and Cardoso (2007), in the same facility with a WES type weir. Recent studies were also conducted by Reis (2015) and Pinto (2017), in which the WES weir was replaced by a piano key weir.

The objective of the present study focused in the characterization of the skimming flow on the stepped chute downstream of a piano key weir, along with the hydraulic jump at the stilling basin.

## 2. General remarks

### 2.1. Piano key weir

The Piano Key Weir (PKW) is a particular case of the traditional labyrinth weir, having a rectangular shape and slopes on both sides, constituting the inlet and outlet keys (Figure 1). The inlet key is the alveoli that is opened to downstream and is sided by two lateral walls and the downstream crest. The outlet key is the alveoli that is opened to the downstream face and is also sided by two lateral walls but by the upstream crest. The extension of the crest in the stretch upstream or downstream is usually called projection. The base structure is made of PKW units, being  $N_u$  the number of units. The unit represents the smallest extension of a complete structure, made by a complete inlet key with two side walls and half of an outlet key on both sides. The main parameters that define the geometry of the PKW are the total width of the weir ( $W$ ), the total developed crest length ( $L$ ), the total length of the weir ( $B$ ) and the total height of the weir ( $P$ ). All of the parameters related to the PKW unit are defined with the index  $u$ , whilst the indexes  $i$ ,  $o$  and  $s$  are associated, respectively, to the inlet key, outlet key and to the side wall. There are four types of PKW known as type A, type B, type C and type D (Figure 1c). The PKW type A designated for the present work includes upstream and downstream projections.

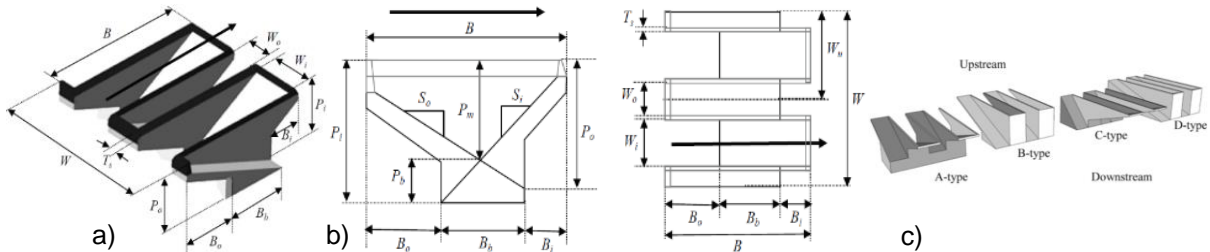


Figure 1 – Representation of a PKW weir: a) 3D view; b) top and side views c) four types of PKW (Pralong et al., 2011, Ercicum et al., 2017).

### 2.2. Residual specific energy

The equivalent clear water depth and the residual specific energy upstream of the hydraulic jump can be estimated through the following hypotheses (Meireles, 2004):

- hypothesis A, considers that in the application of the momentum conservation equation between the upstream and downstream of the hydraulic jump, the distribution of pressures is hydrostatic in the two sections;
- hypothesis B, considers that in the application of the momentum conservation equation between the upstream and downstream of the hydraulic jump, the distribution of pressure is hydrostatic in the downstream section of the hydraulic jump and in the section immediately upstream of the hydraulic jump presents a linear distribution, between zero (free surface) and the value of the piezometric head measured on the stilling basin floor.

For the hypothesis of the hydrostatic pressure distribution (hypothesis A) the momentum conservation equation can be expressed by (Matos, 1999, Meireles, 2004):

$$\gamma \frac{h_{mr}^2}{2} + \alpha' \rho \frac{q^2}{h_{mr}} = \gamma \frac{h_{jr}^2}{2} + \alpha' \rho \frac{q^2}{h_{jr}} \quad (2.1)$$

where  $h_{jr}$  is the flow depth at the end of the hydraulic jump,  $h_{mr}$  is the equivalent clear water depth downstream of the hydraulic jump and  $\alpha'$  the momentum correction coefficient.

For the hypothesis of the linear pressure distribution (hypothesis B) the momentum conservation equation can be expressed by (Meireles, 2004):

$$\gamma h_{mr} \frac{h_{mr}^{piez}}{2} + \alpha' \rho \frac{q^2}{h_{mr}} = \gamma \frac{h_{jr}^2}{2} + \alpha' \rho \frac{q^2}{h_{jr}} \quad (2.2)$$

where  $h_{mr}^{piez}$  is the piezometric head measured in the stilling basin floor upstream of the hydraulic jump.

To determine the flow depth at the downstream end of the hydraulic jump it is necessary to define the end of the hydraulic jump; for this purpose, the criteria presented by Cardoso (2007) was adopted, which is based in obtaining a value less than 5% of the slope between piezometric heads in the bottom of the stilling basin and their distance, which is given by:

$$d_n = \left( \frac{p_{n+1}}{\gamma} + \frac{p_n}{\gamma} \right) / (s_{n+1} - s_n) \quad (2.3)$$

where  $s$  is the distance to the spillway toe and  $p/\gamma$  the piezometric head.

To determine the piezometric head upstream of the hydraulic jump, the maximum value measured in the initial reach of the stilling basin was adopted. When the hydraulic jump begins at the spillway toe, the residual flow energy ( $E_r$ ) can be estimated with the equations (2.4), (2.5) e (2.6) (Manzanares, 1980, Yasuda e Ohtsu, 1999, 2003, *in* Meireles, 2004):

$$E_r = \beta h_{mr} + \alpha \frac{U_{mr}^2}{2g} \quad (2.4)$$

$$\beta = 1 + \frac{1}{\rho g q h_{mr}} \int_0^{h_{mr}} V \Delta p \, dy \quad (2.5)$$

$$U_{mr} = \frac{q}{h_{mr}} \quad (2.6)$$

where  $U_{mr}$  is the average water velocity upstream of the hydraulic jump,  $V$  is the water velocity at a  $y$  distance from the bottom,  $\alpha$  is the kinetic energy coefficient,  $\beta$  is the Jaeger-Manzanares coefficient and  $\Delta p$  is the difference between the real pressure and the pressure from a hydrostatic distribution, at a  $y$  distance from the bottom.

According to Yasuda and Ohtsu (2003), the velocity distribution ( $V$ ) can be calculated by (*in* Meireles, 2004):

$$V = \frac{9}{8} U_{mr} \left( \frac{y}{h_{mr}} \right)^{1/8} \quad (2.7)$$

Considering that the pressure distribution in the upstream section of the hydraulic jump varies linearly between the free surface value and the pressure on the bottom of the stilling basin,  $\Delta p$  can be calculated at the  $y$  distance of the bottom by (Yasuda e Ohtsu 1999, 2003, *in* Meireles, 2004):

$$\Delta p = \rho g (h_{mr}^{piez} - h_{mr}) \left( 1 - \frac{y}{h_{mr}} \right) \quad (2.8)$$

Meireles (2004) obtained values of the kinetic energy coefficient ( $\alpha$ ) and the momentum correction coefficient ( $\alpha'$ ) roughly equal to one, hence the values used herein were  $\alpha = \alpha' = 1$ .

### 3. Experimental set-up

The experiments were conducted in a facility assembled at LNEC, in the framework of previous research works (Matos, 1999, Meireles, 2004, Renna, 2004, Cardoso, 2007, Reis, 2015, Pinto, 2017), which was slightly modified for this study. The experimental facility is divided into five parts: upstream reservoir, piano key weir, stepped spillway, stilling basin and stabilization flume with a Bazin weir. The stepped spillway chute with a piano key weir is 2,96 m (from crest to toe), 1,0 m wide and has a slope of 53° (1V:0,75H). The step height is adjustable; in the present work 4 and 8 cm high steps were used. The stilling basin is 5,0 m long and 1,0 m wide; a total of 67 piezometric taps were installed on the basin

floor and connected to a manometric panel (via plastic tubes) with a resolution of 1,0 mm. The main geometric characteristics of the PKW used in the present research are included in Table 1.

A conductivity probe developed and calibrated by the U.S. Bureau of Reclamation was tested and calibrated to measure the air concentration along the stepped chute. Further details on the instrumentation and the experimental facility can be found in Matos (1999), Meireles (2004) and Reis (2015).

For the study of the flow along the chute, air concentration data were collected in the verticals of the steps (perpendicular to the spillway pseudo-bottom), in the symmetry axes of the inlet and outlet keys, for discharges of 80 and 140 l/s. For the study of the hydraulic jump in the stilling basin Piezometric heads were recorded in all piezometric taps, and flow depths estimated based on visual observation through the plexiglass side walls, for flow rates ranging from 80 to 180 l/s.

Table 1 – Main geometric characteristics of the PKW on the experimental facility.

$W_u$ (m)	$W$ (m)	$L$ (m)	$B$ (m)	$\frac{B_o}{B_i}$	$W_i$ (m)	$W_o$ (m)	$T_s$ (m)	$P$ (m)	$B_i$ (m)	$B_o$ (m)	$\frac{W_i}{W_o}$	$\frac{P}{W_u}$	$\frac{2 T_s}{L}$	$\frac{L}{W}$
0,392	1,000	4,290	0,670	1,000	0,221	0,147	0,012	0,200	0,134	0,134	1,503	0,510	0,014	4,290

Note:  $B$ , total length of the weir;  $B_i$ , length of the inlet key;  $B_o$ , length of the outlet key;  $L$ , total developed crest length;  $P$ , total height of the weir;  $T_s$ , side wall thickness;  $W$ , total width of the weir;  $W_i$ , width of the inlet key;  $W_o$ , width of the outlet key;  $W_u$ , PKW unit width.

## 4. Results

### 4.1. Definitions

The local air concentration ( $C$ ) is defined as the time-averaged value of volume of air per unit volume of air and water. The characteristic flow depth ( $Y_{90}$ ) is defined as the distance to the bottom of the spillway where the air concentration is 90%. The equivalent clear water depth ( $h$ ) is defined as:

$$h = \int_0^{Y_{90}} (1 - C) dy \quad (4.1)$$

where  $y$  is the distance measured normal to the pseudo-bottom. The depth averaged mean air concentration in a given vertical (or in a cross-section, for two-dimensional flow) is calculated with:

$$\bar{C} = \frac{\int_0^{Y_{90}} C dy}{Y_{90}} \quad (4.2)$$

From equations (4.1) e (4.2), the equivalent clear water depth is given as:

$$h = (1 - \bar{C})Y_{90} \quad (4.3)$$

### 4.2. Air concentration distribution

Figures 2 and 3 show the air concentration profiles along the symmetry axes of the outlet and inlet keys, for discharges of 80 l/s (Figure 2) and 140 l/s (Figure 3).

The results show that, regardless of the discharge, the air concentration profiles along the symmetry axes of the outlet and inlet keys are clearly different. Similarly to the results obtained by Reis (2015), for a stepped spillway with 8 cm high steps downstream a PKW weir, the air concentrations originated in the outlet key are higher than those originated in the inlet key. These differences are clearly observed for the discharge of 80 l/s in steps 15, 17 and 19, and for the discharge of 140 l/s in steps 19, 21 and 24. This difference is a result of the highly aerated flow from the outlet key, which leads to a high concentration of air in the initial steps, while in the flow from the inlet key, the aeration only occurs when the jet flow impacts on the stepped chute. The flow from the inlet key reaches the stepped spillway slightly upstream of step 15 for the discharge of 80 l/s, and slightly upstream of step 19 for the discharge of 140 l/s.

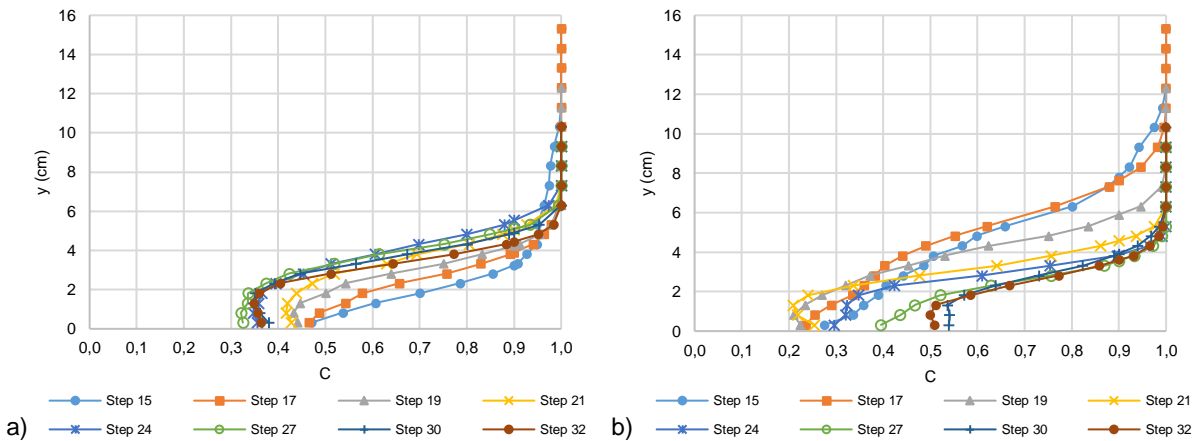


Figure 2 – Air concentration distribution along the chute 4 cm high steps, for  $Q=80$  l/s: a) in the symmetry axis of the outlet key; b) in the symmetry axis of the inlet key.

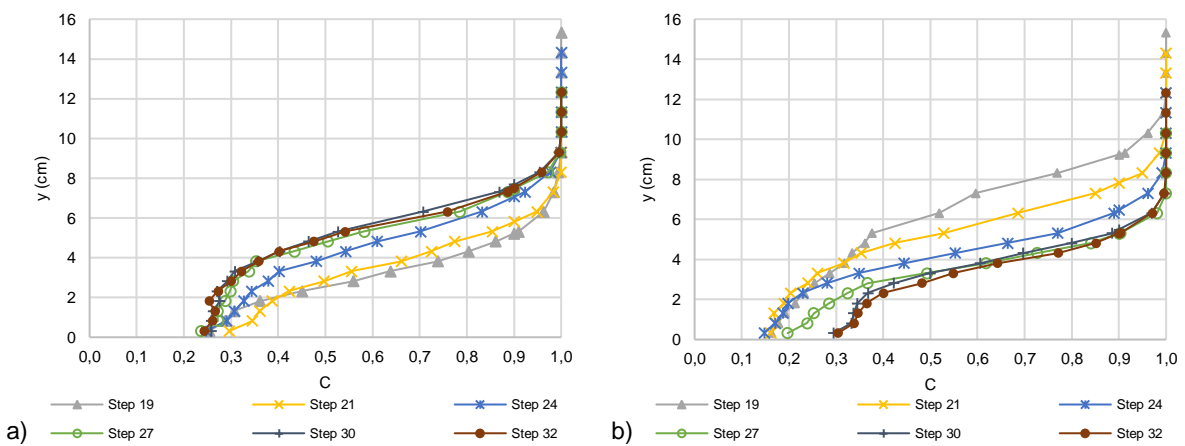


Figure 3 – Air concentration distribution along the chute with 4 cm high steps, for  $Q=140$  l/s: a) in the symmetry axis of the outlet key; b) in the symmetry axis of the inlet key.

#### 4.3. Mean air concentration

Figures 4 and 5 show the mean air concentration ( $\bar{C}$ ) along the spillway, in the symmetry axis of the inlet and outlet keys, for discharges of 80 and 140 l/s.

In Figure 4, data from the present study is shown, along with data from Reis (2015) for the same stepped spillway with 8 cm high steps downstream a PKW weir. The results show that:

- the mean air concentrations measured along the spillway for the discharge flow of 80 l/s, are always larger than those obtained for the discharge of 140 l/s;
- the development trend of the mean air concentration along the spillway is significantly different on the axes of the inlet and outlet keys, and practically independent of the discharge;
- for discharges of 80 and 140 l/s, the mean air concentration obtained by Reis (2015) show the same development trend as those obtained in the present study. In the first three steps, for both discharges, the mean air concentrations from the present study and from Reis (2015) are practically equal, since the flow from the PKW weir is decisive in the initial air concentrations of the spillway. Downstream of the first three steps, the mean air concentration obtained by Reis (2015) gradually increases in relation to the results obtained in the present study, for both symmetry axis.

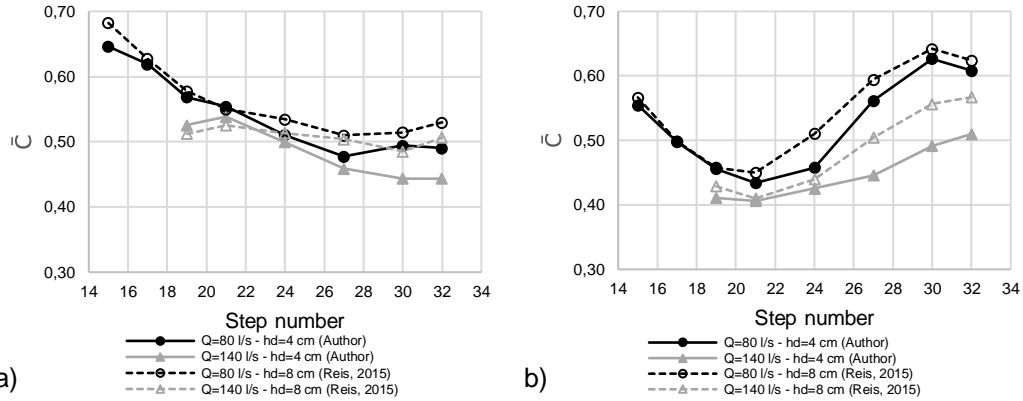


Figure 4 – Mean air concentration along the chute: a) in the symmetry axis of the outlet key; b) in the symmetry axis of the inlet key.

In Figure 5, the mean air concentration data obtained in the present study is plotted, along with those from Meireles (2004) and Matos (1999), for the same stepped chute with 4 and 8 cm high steps, respectively, downstream of a WES weir. The results show that:

- in the initial spillway reach, the mean air concentrations in the symmetry axis of the outlet key are higher than those from the symmetry axis of the inlet key. The difference gradually decreases down the spillway until it reaches steps 24 and 27, for discharges of 80 and 140 l/s respectively; downstream of those steps the development trend changes and the mean air concentrations obtained in the symmetry axis of the inlet key are higher than those of the outlet key. Reis (2015) pointed out that this behaviour is a consequence of the cross-waves and 3D flow downstream of the PKW;
- in the symmetry axis of the outlet key, the mean air concentration tends to decrease down the spillway for both discharges; this trend is different from that observed by Meireles (2004) and Matos (1999) for a WES weir, which shows an increase of the mean air concentration down the spillway. Reis (2015) stated that the intersection of the jets originated from the side walls of the inlet key with the flow from the outlet key results in high turbulence levels, and in the high air entrainment immediately downstream the outlet key;
- for the discharge of 80 l/s, downstream of step 19, the mean air concentration obtained by Meireles (2004) and Matos (1999) are in general between the mean air concentration obtained herein for both symmetry axes; close to the downstream end of the spillway, the mean air concentration obtained by Meireles (2004) is close to that obtained in the symmetry axis of the outlet key;
- for the discharge of 140 l/s, downstream of step 24, the mean air concentration obtained by Meireles (2004) and Matos (1999) are in general between the results obtained in the present study for both symmetry axis.

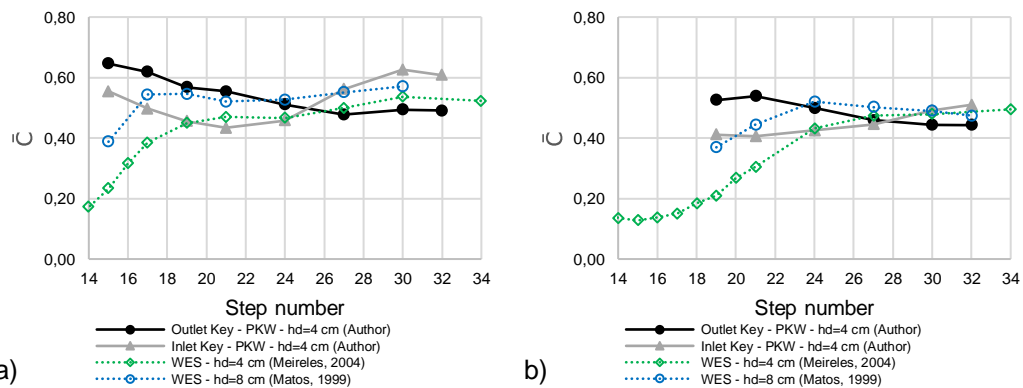


Figure 5 – Mean air concentration along the chute, in the symmetry axes of the outlet and inlet keys: a)  $Q=80$  l/s; b)  $Q=140$  l/s.

#### 4.4. Characteristic flow depths

Figures 6 and 7 show the equivalent clear water depth ( $h$ ) and the characteristic flow depth ( $Y_{90}$ ), respectively, for both symmetry axes, along with results from Reis (2015), for a stepped spillway with 8 cm high steps downstream of a PKW, and from Meireles (2004), for a stepped spillway with 4 cm high steps downstream a WES weir, for discharges of 80 and 140 l/s. From Figures 6 and 7, the following observations can be drawn:

- for both discharges, the values of  $h$  and  $Y_{90}$  in the symmetry axis of the inlet key are initially higher than those for the outlet key, whereas the trend is inverted downstream of steps 21 and 24, for discharges of 80 and 140 l/s, respectively;
- for both discharges, the values of  $h$  and  $Y_{90}$  obtained by Reis (2015) are fairly close to the values obtained in the present study. In the first steps (steps 15 to 19 for discharge of 80 l/s, and steps 19 and 21 for discharge of 140 l/s) the values obtained by Reis (2015) in the symmetry axis of the outlet key are slightly higher than those obtained in the present study;
- for the discharge of 80 l/s, the values of  $h$  obtained by Meireles (2004) are between the results obtained for both symmetry axis along the spillway; the values of  $Y_{90}$  are closer to the results obtained in the symmetry axis of the inlet key, downstream step 21;
- for the discharge of 140 l/s, the values of  $h$  and  $Y_{90}$  obtained by Meireles (2004), downstream step 24, are identical to the results obtained in the symmetry axis of the inlet key.

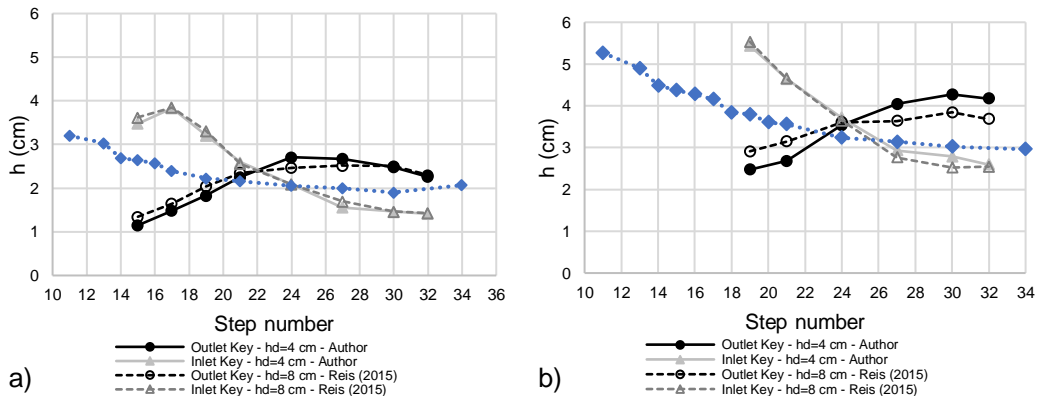


Figure 6 – Equivalent clear water depth along the chute, in the symmetry axes of the inlet and outlet keys: a) Q=80 l/s; b) Q=140 l/s.

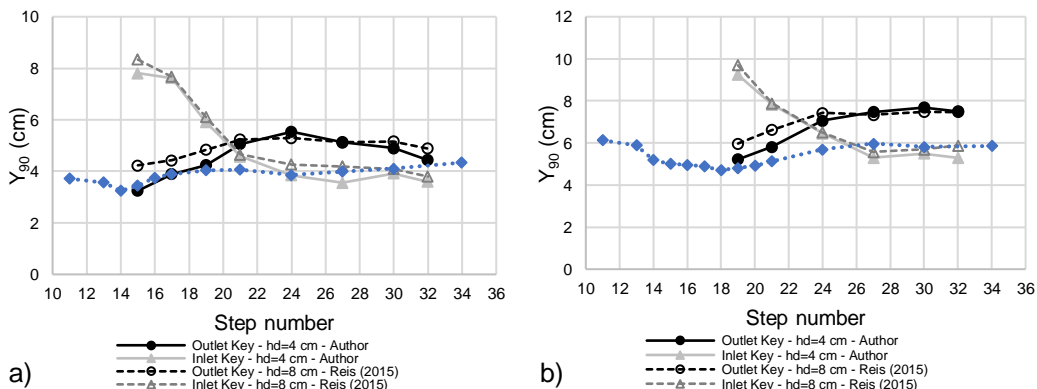


Figure 7 – Characteristic flow depth  $Y_{90}$  along the chute, in the symmetry axes of the inlet and outlet keys: a) Q=80 l/s; b) Q=140 l/s.

#### 4.5. Hydraulic jump in the stilling basin

Figure 8 presents, for discharges from 80 to 180 l/s, the average piezometric heads along the stilling basin floor measured in the present study for a stepped chute with 4 or 8 cm high steps, with the hydraulic jump beginning at the impact point of the flow in the stilling basin. The results show that:

- with the increase of discharge it was possible to observe: *i*) an increase of the piezometric heads in the stilling basin; *ii*) an offset of the maximum piezometric head in the impact section, to downstream;

iii) the piezometric heads downstream the hydraulic jump tends to stabilize at a longer distance from the toe of the spillway;

- the piezometric heads downstream of the hydraulic jump obtained for 4 cm high steps are close to the values obtained for 8 cm high steps; however, for discharges higher than 100 l/s, the piezometric heads obtained for 4 cm high steps are slightly higher than those obtained with 8 cm high steps.

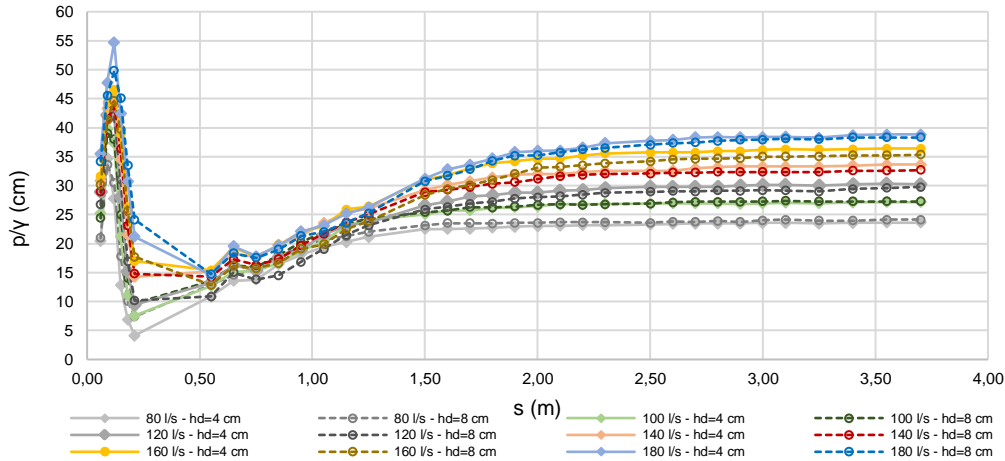


Figure 8 – Piezometric heads along the stilling basin with the hydraulic jump starting at the impact point of the flow in the stilling basin.

#### 4.6. Equivalent clear water depth upstream of the hydraulic jump

In Figures 9 to 12 it is shown the results obtained in the present study for a stepped chute with 4 and 8 cm high steps downstream of a PKW weir, and results from Meireles (2004), for a stepped chute with 4 and 8 cm high steps downstream of a WES weir.

In Figure 9 is shown the equivalent clear water depth upstream of the hydraulic jump for the hypothesis A (hydrostatic pressure distribution, Equation 2.1) and for the hypothesis B (linear pressure distribution, Equation 2.2). The results show that:

- the equivalent clear water depths upstream of the hydraulic jump obtained with 4 cm high steps are generally slightly lower than those obtained with 8 cm high steps (for the same type of weirs);
- the equivalent clear water depths upstream of the hydraulic jump obtained with PKW weirs are slightly lower than those obtained with WES weirs (for same step height).

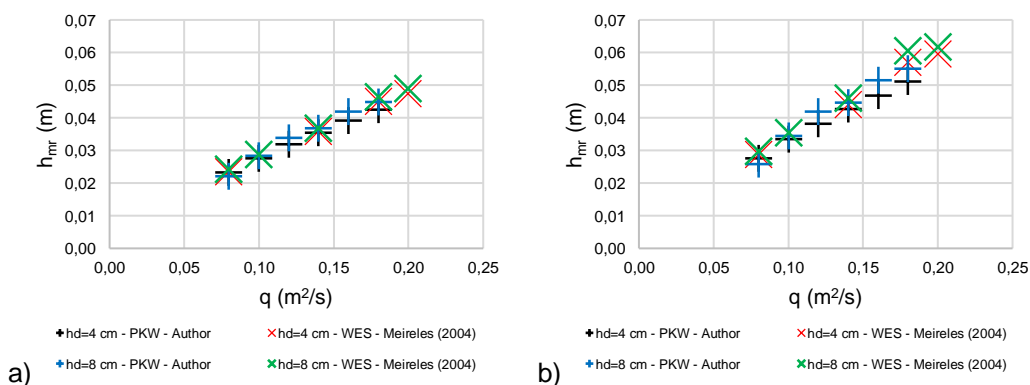


Figure 9 – Equivalent clear water depth at the upstream section of the hydraulic jump: a) hypothesis A; b) hypothesis B.

In Figure 10 it is shown the ratio between the equivalent clear water depth upstream of the hydraulic jump, obtained through hypothesis A and B ( $h_{mrB}/h_{mrA}$ ), in function to the ratio between the critical depth and step height ( $h_c/h_d$ ). In analogy to the results obtained by Meireles (2004), the ratio  $h_{mrB}/h_{mrA}$  virtually doesn't change with  $h_c/h_d$ . The same conclusion can be obtained for the ratio  $E_{rB}/E_{rA}$ . The following regression equations were obtained from the data related to the PKW weir (Equations 4.4 and 4.5) and for the data related to both weirs (Equations 4.6 and 4.7):

$$h_{mrB}/h_{mrA} = 1,207 \quad (\text{PKW}) \quad (4.4)$$

$$E_{rB}/E_{rA} = 0,765 \quad (\text{PKW}) \quad (4.5)$$

$$h_{mrB}/h_{mrA} = 1,226 \quad (\text{PKW and WES}) \quad (4.6)$$

$$E_{rB}/E_{rA} = 0,757 \quad (\text{PKW and WES}) \quad (4.7)$$

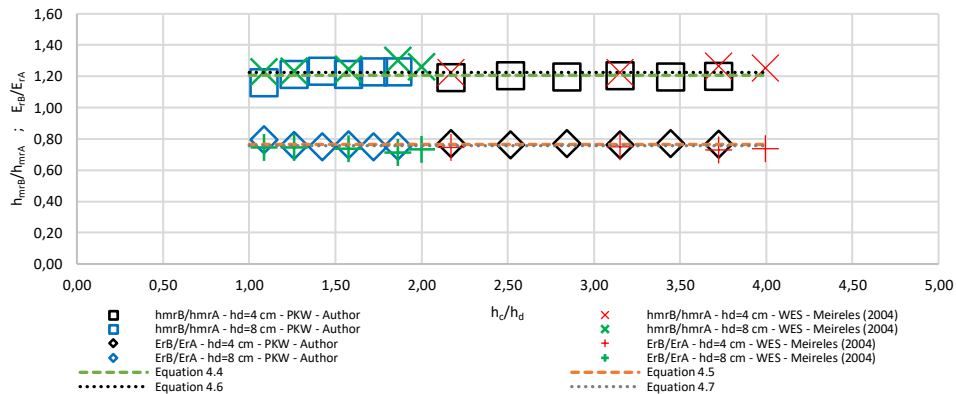


Figure 10 – Influence of applying hypothesis A or B on the equivalent clear water depth and residual specific energy.

Applying hypothesis A to calculate the equivalent clear water depth and the residual specific energy upstream of the hydraulic jump, leads to an underestimation of approximately 18% of the equivalent clear water depth and an overestimation of approximately 32% of the residual specific energy, in comparison to the results obtained by applying hypothesis B.

For situations where it is only possible to measure the water depth downstream of the hydraulic jump it is useful to use equations (4.4) to (4.7), which allow to estimate, in the tested range of values of  $h_c/h_d$ , the equivalent clear water depth and the residual specific energy at the spillway toe of stepped spillways with the same relative step height, identical slope and same type of weirs.

#### 4.7. Energy dissipation

In Figure 11 it is shown the dimensionless energy dissipation at the spillway ( $\Delta H/h_c$ ) in function to the relative dam height ( $H_d/h_c$ ), both normalized by the critical depth.

The energy dissipation at the spillway with 4 cm high steps downstream a PKW weir was slightly lower than that for a spillway with the same step height downstream a WES weir (mean relative difference of -2,0%, for hypothesis B).

The energy dissipation at the spillway with 4 cm high steps downstream of a PKW weir was generally slightly lower than that at the spillway with 8 cm high steps downstream of a PKW weir (mean relative difference of -2,0%, for hypothesis B).

The following regression equations were found to fit well to the data obtained through the hypothesis B for PKW weirs, WES weirs and both weirs:

$$\Delta H/h_c = 0,896 H_d/h_c - 2,712 ; R^2 = 0,994 \quad (\text{PKW}) \quad (4.8)$$

$$\Delta H/h_c = 0,930 H_d/h_c - 2,717 ; R^2 = 0,998 \quad (\text{WES}) \quad (4.9)$$

$$\Delta H/h_c = 0,901 H_d/h_c - 2,455 ; R^2 = 0,989 \quad (\text{PKW and WES}) \quad (4.10)$$

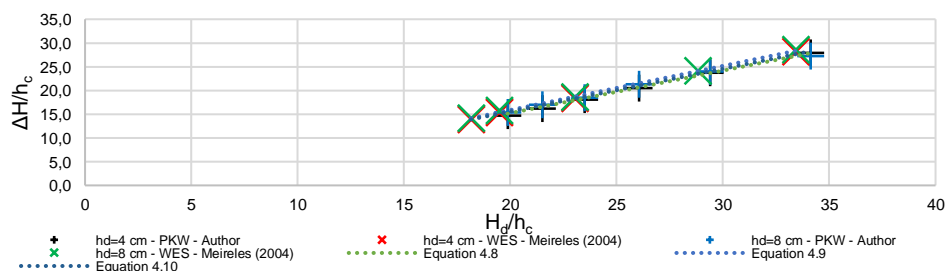


Figure 11 – Dimensionless energy dissipation at the spillway in function to the relative dam height (hypothesis B).

## 5. Conclusions

The purpose of the present study was to provide a contribution to the research on the main flow properties of a stepped spillway downstream of a piano key weir.

For the skimming flow study in the stepped spillway, the following conclusions can be drawn:

- For both discharges, the mean air concentration values obtained by Reis (2015) show the same trend along the spillway as the values obtained in the present study; in the first three steps (for both discharges), the mean air concentrations are identical in both studies, whereas further downstream, the mean air concentration values obtained by Reis (2015) gradually increase in relation to those obtained in the present study;
- for the discharge of 80 l/s and downstream step 19, the mean air concentration values obtained by Meireles (2004) and Matos (1999) are generally between the values obtained in the present study for the symmetry axes of the outlet and inlet keys, although the mean air concentration values obtained by Meireles (2004) are closer to the values obtained in the last steps of the symmetry axis of the outlet key;
- for the discharge of 140 l/s and downstream step 24, the mean air concentration values obtained by Meireles (2004) and Matos (1999) are practically between the values obtained in the present study for the symmetry axes of the outlet and inlet keys;
- for both discharges, the values of  $h$  and  $Y_{90}$  obtained by Reis (2015) are fairly close to the values obtained in the present study;
- for the discharge of 80 l/s, the values of  $h$  obtained by Meireles (2004) are between the results obtained for both symmetry axis along the spillway; the values of  $Y_{90}$  are closer to the results obtained in the symmetry axis of the inlet key, downstream step 21;
- for the discharge of 140 l/s, the values of  $h$  and  $Y_{90}$  obtained by Meireles (2004), downstream of step 24, are identical to the results obtained in the symmetry axis of the inlet key.

With regard to the study of the hydraulic jump in the stilling basin, the following conclusions can be drawn:

- the piezometric heads downstream of the hydraulic jump obtained for 4 cm high steps are close to the values obtained for 8 cm high steps; however, for discharges higher than 100 l/s, the piezometric heads obtained for 4 cm high steps are slightly higher than those obtained with 8 cm high steps;
- the equivalent clear water depths upstream of the hydraulic jump obtained with 4 cm high steps are generally slightly lower than those obtained with 8 cm high steps (downstream of the same type of weirs), and the equivalent clear water depths upstream of the hydraulic jump obtained with PKW weirs are slightly lower than those obtained with WES weirs (for the same step height);
- The energy dissipation at the spillway with 4 cm high steps was generally slightly lower in relation to the energy dissipation with 8 cm high steps (downstream of the same type of weirs), and the energy dissipation at the spillway downstream a PKW weir was slightly lower when compared with the energy dissipation for a spillway with the same step height downstream a WES weir;
- Normalized formulae were proposed to estimate the head loss on stepped spillways downstream of PKW and WES weirs.

## Acknowledgements

The author thankfully acknowledges Professor Jorge Matos (IST) and Dr. Maria Teresa Viseu (LNEC) for all the supervision and support of the M.Sc. thesis.

## References

- Cardoso, G. (2007). Ressonância hidráulica em bacias de dissipação com acessório a jusante de descarregadores de cheias em degraus. Estudo experimental. Dissertação de mestrado, Instituto Superior Técnico, Lisboa, Portugal (in portuguese).
- Epicum, S., Archambeau, P., Dewals, B. & Piroton, M. (2017). Hydraulics of Piano Key Weirs: A review. Labyrinth and Piano Key Weirs III PKW 2017, Epicum et al. (Eds), pp. 27-36.
- Manzanares, A. A. (1980). Hidráulica Geral. Técnica, AEIST, Vol. 2, Lisboa, Portugal (in portuguese).
- Matos, J. (1999). Emulsão de ar e dissipação de energia do escoamento em descarregadores em degraus. Dissertação de doutoramento, Instituto Superior Técnico, Lisboa, Portugal (in portuguese).
- Meireles, I. (2004). Caracterização do escoamento deslizante sobre turbilhões e energia específica residual em descarregadores em degraus. Dissertação de mestrado, Instituto Superior Técnico, Lisboa, Portugal (in portuguese).
- Meireles, I. (2011). Hidráulica dos descarregadores em degraus: estudo experimental-numérico-teórico. Dissertação de doutoramento, Universidade de Aveiro, Aveiro, Portugal (in portuguese).
- Pinto, M. (2017). Dissipação de energia em descarregadores de cheias em degraus com soleira em teclado de piano: estudo experimental. Dissertação de mestrado, Instituto Superior Técnico, Lisboa, Portugal (in portuguese).
- Pralong, J., Vermeulen, J., Blancher, B., Laugier, F., Epicum, S., Machiels, O., Piroton, M., Boillat, J-L., Leite Ribeiro M. & Schleiss, A. (2011). A naming convention for the Piano Key Weirs geometrical parameters. Labyrinth and Piano Key Weirs PKW 2011, pp. 271-278.
- Reis, M. (2015). Estudo experimental do escoamento em descarregadores de cheias em degraus com soleira em teclado de piano. Dissertação de mestrado, Instituto Superior Técnico, Lisboa, Portugal (in portuguese).
- Renna, F. (2004). Caratterizzazione Fenomenologica del Moto di un Fluido Bifasico Lungo Scaricatori a Gradini. Tese de doutoramento, Politécnico de Bari, Cosenza, Italy (in italian).
- Yasuda, Y., Ohtsu, I. (1999). Flow resistance of skimming flow in stepped channels. Proc. 28th IAHR Congress, Theme B, B14, Graz, Austria.
- Yasuda, Y., Ohtsu, I. (2003). Effect of step cavity area on flow characteristics of skimming flows on stepped chutes. Proc. 30th IAHR Congress, Theme D, IAHR, Salonica, Greece, pp. 703-710.